

Method of Determination of Technological Durability of Plastically Deformed Sheet Parts of Vehicles

Volodymyr Dragobetskii^{1*}, Mykhaylo Zagirnyak¹, Olena Naumova¹,
Sergii Shlyk¹, Aleksandr Shapoval²

¹Kremenchuk Mykhailo Ostrohradskyi National University

²Scientific Production Association "Tungsten"

*Corresponding author E-mail: vldrag@kdu.edu.ua

Abstract

The purpose of the article is to develop an apparatus providing maximum or predicted durability of parts treated during their manufacture by plastic deformation. In these terms, the parameters of the technological process should provide the maximum or expected increase of the endurance limit in comparison with the initial parts values before the strengthening by the surface plastic deformation or after plastic forming. The article describes the influence of the degree of preliminary deformation on the kinetics of fatigue failure of metals and alloys. Experimental data of the ultimate deformations of welded workpieces were obtained, which make it possible to evaluate the manufacturing of parts with a weld seam at the design stage of the technological process. The developed method made it possible to determine the nonstationary field of stresses in the deformation region, ultimate deformations and the most rational scheme of the stress-strain state, which excludes the localization of deformations and destruction of the weld zone of a welded cylindrical workpieces.

Keywords: cylindrical workpiece; deformation; durability; strengthening; weld seam; wheel rim.

1. Introduction

Reliable and safe operation of machine parts and engineering structures in the various operating conditions is largely determined by the structure and properties of the materials used for their manufacture. To improve the structure and properties of the raw materials, various technological processes for their pretreatment are used. In particular, welding, the volume and the surface plastic deformation (SPD).

SPD as rolling by balls and rollers, grit blasting, diamond smoothing, cavitation in alkaline environment, vibration grinding, etc. is one of the most common and effective technological methods for increasing the machine parts and mechanisms resource.

According to present views, of a large number of factors affecting to the fatigue resistance of welded joints the most important are the stress concentration around the different ledges, pores and notches and residual stresses, the value of which can even exceed the yield strength of the material, and, therefore, significantly reduce the safety margin of welded products. The most effective technological ways of increasing the cyclic durability of welded joints are the heat treatment and SPD of the seam material and the weld zone. According to [1], the hardening of the weld can significantly increase the fatigue resistance. Thus, if the previously considered [2] that the durability of the welded joint is determined mainly by the cracks proliferation after welding since the significant defects after welding remain leading to the elimination of the crack initiation step, in [3] shown the basic and, perhaps, the dominant role of the stage of its formation.

The published data on the effects of cold plastic deformation resistance to fatigue failure is very limited and contradictory. The discrepancy between the experimental data is determined by the dependence of the fatigue resistance to the degree of preliminary

plastic deformation. However, information about this is rare and has a random character. Based on the analysis of literature data, it could be concluded that the SPD, as a rule, leads to an increase of the materials resistance to the fatigue due to the compaction of the surface layers and the residual compressive stresses appearance in them. A particularly significant increase of fatigue properties is observed after the friction-strengthening types of surface treatment when forming a structure of the "white layer" – a thin secondary quench layer consisting of a mixture of finely dispersed needled martensite and austenite and very fine precipitates of Fe_xC-type carbides.

In connection with this and with taking into account the intensive development of progressive methods of volumetric and surface plastic deformation, the task of increasing the operational durability of deformation-hardened steels and their welded joints with a decrease of the metal consumption of products is very relevant.

The studies were carried out on the steels and their welded joints that are widely used in the automotive and other industries. Samples were preliminarily deformed with a degree of deformation $\varepsilon = 0...29\%$ with a strain rate of $2 \cdot 10^{-3} \text{ s}^{-1}$. The optimum processing time was determined from the distribution patterns and the magnitude of the axial residual compressive stresses.

2. Research Methods

2.1. Determination of the Destructive Deformations

The definition of destructive deformations can be carried out in several ways. To determine the deformations at which the welded cylindrical workpiece collapses (welded seam is located along the generatrix) it is possible to use a semi-empirical approach, which is based on the extrapolation of deformations obtained by stepwise

loading of the samples. The block diagram is presented on the Fig. 1.

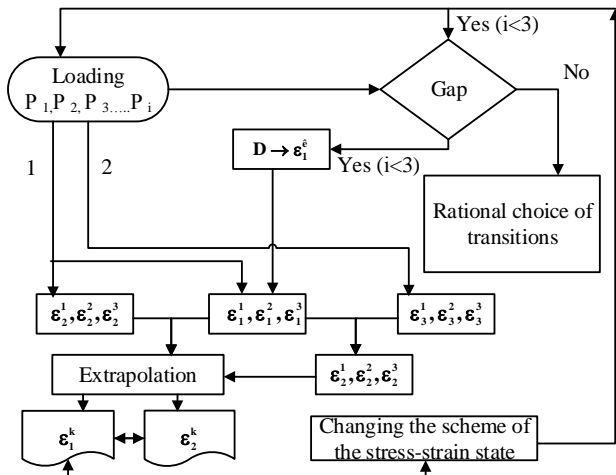


Fig. 1: Block diagram of the destructive deformations determination.

In this case, the workpiece is loaded at least by three forming operations before failure. After each operation the achieved deformations $\epsilon_1, \epsilon_2, \epsilon_3$ and the current workpiece diameters up to which the spreading or crimping carried out are measured. The obtained diameters are plotted on the graph in Fig. 2 and the deformations are on the graph in Fig. 3.

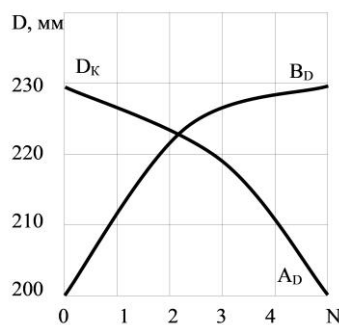


Fig. 2: Dependence of diameters and deformations of samples by steps.

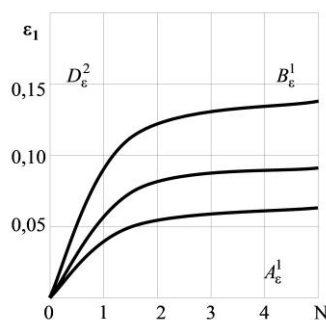


Fig. 3: Dependence of deformations of samples by steps.

The subsequent extrapolation of the curves for diameters determines the step number at which the workpiece reaches the required size and the corresponding extrapolation of deformations determines the level of the necessary step, at which the values of ϵ_1 and ϵ_2 are corresponding to the required spreading diameter of the workpiece. These deformations must be compared with the diagram of the ultimate strains. If the obtained deformations are in the stamping area, then no special technological methods are necessary. Therefore, it is sufficient to make a rational choice of the number of steps. In practice, when carrying out similar experiments, it is accessible and simple to measure diameters and from here – to measure circumferential deformations ϵ_1 and thinnings ϵ_3 . Those, to clarify the method of calculating the parameters of the ultimate shape change, it is expedient to carry out experiments for determining the ultimate deformations in the spreading of

welded cylindrical workpieces and to develop a method for determining the destructive deformations and localizations of deformations preceding destruction.

Considering that at present, a number of methods that making it possible to obtain information on how it is necessary to influence on workpieces in order to increase the permissible deformation degrees have been developed, it is quite appropriate to use the obtained results for the analysis in theoretical studies.

As a criterion for estimating the ductility of a metal under a plane stressed state and the dependence of plasticity to the stress state scheme, it is expedient to use the stress state index when the average stress is zero ($\sigma_2 = 0$) [4]:

$$\eta = \frac{2\mu_\sigma}{\sqrt{\mu_\sigma^2 + 3}} \quad (1)$$

And in the case of flat compression:

$$\eta = \frac{\mu_\sigma + 3}{\sqrt{\mu_\sigma^2 + 3}} \quad (2)$$

where η – stress state index;

μ_σ – Lode-Nadai coefficient.

2.2. Analysis of Defects of Welded Cylindrical Workpieces at the Radial-Rotational Profiling Of Wheel Rims

In the automotive, aviation, shipbuilding and instrument-making industries, items obtained by the methods of plastic deformation from welded cylindrical workpieces are widely used. For the formation of wheel rims is using the butt welding. The workpiece is usually rolled with straight ends. After deburring and removing of the planted metal from the outer and inner sides of the rim, it is calibrated in special devices. First, the rim is evenly stretching in the expander and then crimping to a specified size. Rim with poor-quality welding is usually destroyed in the expander. At the same time, the high quality of welding does not guarantee the formation of cylindrical workpieces without destroying the weld seam and the weld zone.

All the defects encountered during butt welding of cylindrical workpieces are proposed to be divided into three groups [5]:

- irregularity of the geometrical shape of the welded assembly;
- macrostructure defects;
- microstructure defects.

The defects of the first group include the displacement of the section symmetry axis, the difference in the geometry of the sections to be joined, the skew, the different thicknesses of the welded surfaces (ends of the cut of welded workpiece). The presence of these defects causes a decrease in the strength of the welded structure. The displacement and misalignment of the jointed sections are caused by inaccurate workpiece preparation, improper installation in the electrodes, insufficiently rigid attachment, significant gaps in the guide machine and low stiffness of the frame.

The main defects of the second and third group are low-quality welding, stratification, cracks, friability, coarse grain structure, pollution of the joint with non-metallic inclusions and microcracks. These defects in the manufacturing of the wheel rims are virtually eliminated and there is no point in considering them.

The value of the defective wheel rims connected with the welded joint and the weld zone material discontinuity is up to 29 – 37 %. Of this number, up to 80 % account to the break in weld seam (Fig. 4), about 17 – 19 % to the fracture of the weld zone (Fig. 5), about 2 – 3 % to the combined gap when the continuity of the welded joint and the weld zone is broken simultaneously (Fig. 6). The breaking of the workpiece basic material (Fig. 7) occurs rarely.



Fig. 4: The weld seam rupture on the wheel rim.



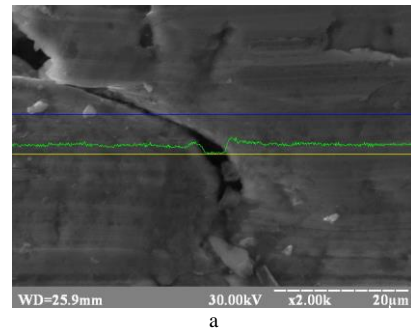
Fig. 5: The weld zone rupture in the wheel rim.



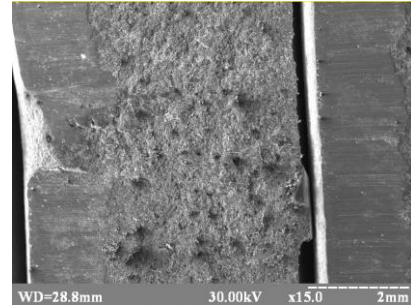
Fig. 6: Combined rupture of the weld seam and the weld zone.



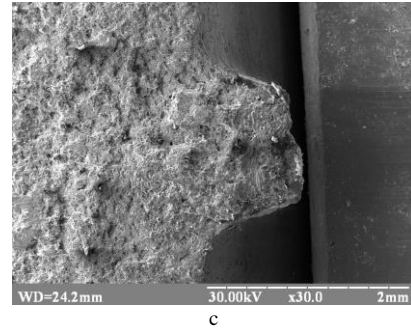
Fig. 7: Breaking of the workpiece basic material.



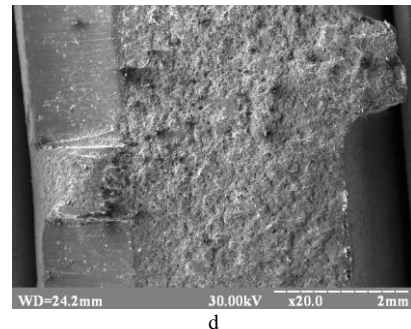
a



b



c



d

Fig. 8: Defects of welded surfaces after cutting on guillotine shears.

To determine the causes of defects, the following analysis methods were used: macroscopic, microscopic, fractographic. Micro- and fractographic analysis was carried out using an electron microscope which is a tool for measuring linear dimensions in the range of 0.1 – 5000 µm with resolution ability in high vacuum secondary electrons of 4 nm.

As a result of the analysis it is established:

- the absence of a thermal influence zone during the formation of a weld seam at the end of the workpiece;
- presence of the cold cracks at the point of a weld seam rupture (Fig. 8, a);
- the absence of weld and the presence of the end cracks after welding at the end of the workpiece (Fig. 8, b);
- quasi-cleavage as micromechanism of the weld failure (Fig. 8, c);
- combination of peeling separation and stratification along the slip planes as micromechanism of the workpiece end destruction (Fig. 8, d).

In addition to the microscopic analysis of the weld seam and the weld zone fractures, the jointed sections before welding were considered. At the ends of the jointed sections after cutting on guillotine shears cracks appeared. The presence of cracks arising during the workpieces cutting aggravates the unfavorable conditions of deformation of the workpiece locations that have been mostly subjected to destruction and, eventually, the operational reliability of the wheel rim.

3. Theoretical Research

3.1. Calculation of the Welded Workpieces Forming Process with Taking into Account the Deformations Localization of Preceding Fracture

In the theoretical analysis of the workpiece deformation in the process of radial-rotational profiling, three aspects can be identified:

- dynamic – shows the ratio of the stress tensor component arising during the workpiece deformation and rotation with the displacement vector;
- geometric – which is corresponding to the deformation and finite displacements ratio;
- physical – determines the components of the strain and stress tensors ratio.

These three aspects are described by equations which together with the initial and boundary conditions are a closed system. For the solving of the problems of rotating workpieces plastic deformation the analytical solution of the system of equations is rather complicated. Therefore, there are necessary to turn to its numerical solution [6].

Consider the basic assumptions. The workpiece is the thin-walled shell. The criterion for the destruction of a welded workpiece is the achievement of ultimate strains in the weld seam corresponding to the ultimate stresses and the boundary value of the stress state index.

The data for calculating of the wheel rim profiling process, physical and mechanical properties of the materials satisfying the requirements of the profiling process for steels 08kp and 08ps (analogue in the U.S. – steels 1008 and 1010, analogue in the EU – steels DC01 and DD13) are shown in Table 1.

Table 1: Physical and mechanical properties of the wheel rims material

Physical and mechanical properties	Steel grade	
	Steel 08kp	Steel 08ps
σ_T , MPa	226	262
σ_B , MPa	334	336
σ_T / σ_B , MPa	0.67	0.75
δ_N , %	26.2	24.9
HRB, MPa	≥ 42	≥ 42
σ_Y , MPa	408	411
ε_i	0.217	0.26
a_0	> 1.2	> 1.2
a_1	> 1.5	> 1.5
δ_R , %	42.9	34.6

Note: σ_T and σ_B – yield and strength limits; δ_R and δ_N – relative elongations at the rupture and the sample uniform stretching at the time of neck formation; HB – Brinell hardness index; σ_Y and ε_i – the true ultimate strength (critical stress) and the logarithmic deformation degree at the time of the neck formation onset with the sample uniform stretching; a_0 and a_1 – anisotropy coefficient in the longitudinal and transverse directions.

The calculation method is based on the representation of the entire shell in the form of a grid model. The workpiece is divided into sections; the mass of each site is reduced to the point; the resulting nodes are connected by weightless extensible links that remain straight between mass concentration points; the external forces are considered as concentrated at each mass point [7].

Fig. 9 shows the scheme for the workpiece splitting into sections in a cylindrical coordinate system.

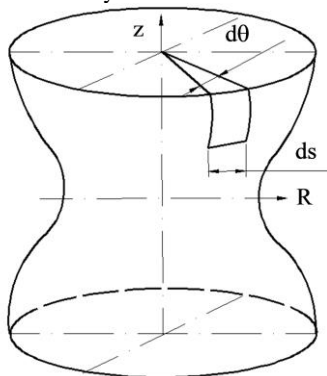


Fig. 9: The scheme of the workpiece splitting into sections in a cylindrical coordinate system.

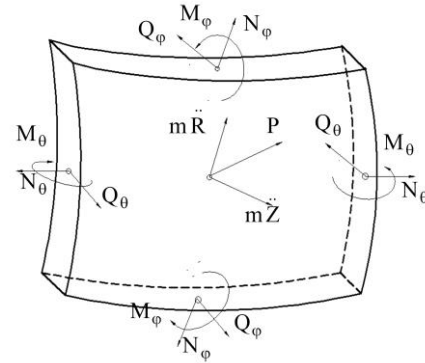


Fig. 10: The forces acting on the shell element.

In accordance to the adopted model, which allows solving equations in finite difference form, the entire bend is concentrated at the mass location points.

Equations of motion in the finite difference form have the form:

$$N_{\varphi i} R_i \cos \varphi_i - N_{\varphi i-1} R_{i-1} \cos \varphi_{i-1} - Q_{\varphi i} R_i \sin \varphi_i + \quad (3)$$

$$+ Q_{\varphi i-1} R_{i-1} \sin \varphi_{i-1} - N_{\varphi} \Delta S_i + P(t)_i R_i \Delta S_i - \rho_i R_i \ddot{R}_i \Delta S_i = 0,$$

$$N_{\varphi i} R_i \sin \varphi_i - N_{\varphi i-1} R_{i-1} \sin \varphi_{i-1} + Q_{\varphi i} R_i \cos \varphi_i - \quad (4)$$

$$- Q_{\varphi i-1} R_{i-1} \cos \varphi_{i-1} + P(t)_i Z_i \Delta S_i - \rho_i R_i \ddot{Z}_i \Delta S_i = 0.$$

where $P(t)_i$ – external load on the i -th element of the shell.

The mesh acceleration in the median plane, its velocity and displacement is determined from the equilibrium equations developed by the authors for each node of the workpiece:

$$\begin{aligned} \nabla_{\gamma} M_{mn}^{\beta\alpha} - Q_{mn}^{\beta} R_{\gamma mn}^{\beta} + P_{mn}^{\alpha} + T_{mn}^{\alpha} + S_{mn}^{\alpha} &= \bar{\rho} \ddot{X}_{mn}^{\alpha} - \rho \dot{X}_{mn}^{\alpha} c, \\ M_{mn}^{\beta\alpha} R_{\beta\alpha}^{mn} + \nabla_{\beta} Q_{\beta}^{mn} + P_{mn}^3 + T_{mn}^3 + S_{mn}^3 &= \rho \ddot{X}_{mn}^3 - \rho \dot{X}_{mn}^3 c, \end{aligned} \quad (5)$$

$$\nabla_{\beta} L^{\alpha\beta} - Q_{mn}^{\alpha} = 0,$$

where ∇_{β} – the sign of a covariant differentiation; M_{mn} – membrane forces; L – bending moments; Q_{mn}^{β} – cutting forces; $\bar{\rho}$ – reduced weight; \ddot{X}_{mn}^j – acceleration; P_{mn}^j – force effect of loading; T_{mn} – friction forces in the peripheral zone of the workpiece; S_{mn} – braking forces of the resistance elements; P_{mn} – forces acting in the workpiece from the elements of resistance; R_{mn} – tensor of curvature; c – soundspeed in the environment.

The value of forces and moments acting on each element determined by the system of equations:

$$\begin{cases} M_{mn}^{\alpha\beta} = \int_{-0.5\delta}^{+0.5\delta} \left[\sigma_{\alpha_1}^{mn} (\delta_1^{\beta} - x^3 B_{1mn}^{\beta}) + \right. \\ \left. + \sigma_{\alpha_2}^{mn} (\delta_2^{\beta} - x^3 B_{2mn}^{\beta}) \right] (G_{mn} \cdot A_{mn}^1)^{0.5} dx \\ L_{mn}^{\alpha\beta} = \int \left[\sigma_{\alpha_1}^{mn} (\delta_1^{\beta} - x^3 B_{1mn}^{\beta}) + \right. \\ \left. + \sigma_{\alpha_2}^{mn} (\delta_2^{\beta} - x^3 B_{2mn}^{\beta}) \right] \cdot (G_{mn} \cdot A^{-1})^{0.5} x^3 dx \\ Q_{mn}^{\alpha} = \frac{\partial L_{mn}^{\alpha\beta}}{\partial x^{\beta}} + \bar{A}_{mn}^{\alpha} \cdot \frac{\partial \bar{A}_1^{mn}}{\partial x^{\beta}} \cdot L_{mn}^{\gamma\beta} + \bar{A}_{mn}^{\beta} \cdot \frac{\partial \bar{A}_r^{mn}}{\partial x^{\beta}} \cdot L_{mn}^{\alpha\beta} \end{cases} \quad (6)$$

The acceleration of the grid nodes of the workpiece median surface in the next field of integration should be determined by equation:

$$\ddot{x}_{mn}^j = \frac{A_{mn}^{0,5}}{\bar{\rho}_o} \cdot (P_{mn}^j + T_{mn}^j + S_{mn}^j + \Pi_{mn}^j) + \frac{A_{mn}^{0,5}}{\bar{\rho}_o} \cdot \left(\frac{\partial V_{mn}^{\beta j}}{\partial x^\beta} + \bar{A}_{mn}^\beta \cdot \frac{\partial \bar{A}_\gamma^{mn}}{\partial x^\beta} \cdot V^{\gamma j} \right), \quad (7)$$

where A_{mn} – the determinant of the metric tensor; $V_{mn}^{\alpha j}$ – space-surface tensor.

The time interval Δt is chosen from the stability condition of the computational process [8]:

$$\Delta t \leq \Delta X_{5,j,0} \left[\rho_3 (1 - \nu_k)^2 (E)^{-1} \right]^{0,5}, \quad (8)$$

where ρ_3^k – the density of the workpiece material; ν_k – Poisson's ratio; E – Young's modulus of the workpiece material.

After determining the coordinates of the points, it is possible to calculate the strain values at the nodes along the layers:

$$\varepsilon_0^{ij} = \frac{(R_i - R_{oi})}{R_{oi}} = \frac{\nu_0 \Delta \varphi_i}{\omega R_{oi}}, \quad (9)$$

$$\varepsilon_z^{ij} = (\Delta S_i - \Delta S_{oi}) \Delta S_{oi} - f_k \frac{\Delta \varphi_i - \Delta \varphi_{oi}}{0,5(\Delta S_{oi+1} - \Delta S_i)}, \quad (10)$$

where ε_0^{ij} – latitudinal deformation;

ε_z^{ij} – meridional deformation;

$\Delta \varphi_i$ – the angle between the links i and $i+1$;

o – an index indicating that the value is determined in the non-deformable state of the structure;

ω – angular speed of roller rotation;

ν_0 – feed speed of profiling roller;

f_k – the distance of the layer from the neutral axis, which is determined by formula:

$$f_k = \delta(i - 0,5(k+1)) / k, \quad (11)$$

where δ – shell thickness;

k – number of layers;

i – layer number.

After determining the values of deformations at each node and in each layer, proceed to the solution of the physical side of the problem - calculating the values of σ_0^{ij} and σ_z^{ij} . In this case, the workpiece material is generally considered to be elastic-plastic, strain and kinematically hardening. Calculations of deformations stresses are based on the dependences of the mathematical theory of plastic flow:

$$\sigma_0^{i,j+1} = \sigma_0^{ij} + \frac{E}{1+\mu^2} (\Delta \varepsilon_0^{i,j+1} + \mu \varepsilon_z^{i,j+1}), \quad (12)$$

$$\sigma_z^{i,j+1} = \sigma_z^{ij} + \frac{E}{1+\mu^2} (\Delta \varepsilon_z^{i,j+1} + \mu \varepsilon_0^{i,j+1}), \quad (13)$$

where μ – Poisson's ratio;

σ_z and σ_θ – meridional and latitudinal stresses;

E – workpiece elastic modulus.

Equations to calculate the forces and moments:

$$N_\phi^{i,j+1} = \sum_{i=1}^k \sigma_z^{i,j+1} \delta_e, \quad N_\theta^{i,j+1} = \sum_{i=1}^k \sigma_\theta^{i,j+1} \delta_e, \quad (14)$$

$$M_\phi^{i,j+1} = \sum_{i=1}^k \sigma_z^{i,j+1} \delta_e f_k, \quad M_\theta^{i,j+1} = \sum_{i=1}^k \sigma_\theta^{i,j+1} \delta_e f_k, \quad (15)$$

where δ_e – the current thickness of the plate layer, defined as

$$\delta_e = \exp(\varepsilon_z) \delta_{oi}. \quad (16)$$

where δ_{oi} – initial thickness of the plate layer.

The magnitude of the shear force Q_ϕ is determined from the equation of moments equilibrium:

$$\frac{d(M_\phi R)}{ds} - M_\theta \cos \phi = Q_\phi R. \quad (17)$$

Then the cycle (9 – 17) is repeated until the moment when the plastic properties of the material, predominantly in the weld zone, approach to the limits for which at each step we compare the current strain values with the ultimate ones. This technique allows to stamp parts at large values of the main deformations, but its possibilities are limited.

On the Fig. 11 is shown that form change occurs only when the point C corresponding to the deformations on the cylindrical workpiece is located inside the area bounded by the points ABD . The abscissa of the current deformation point C , which is above the curve of ultimate deformations BD , should not exceed the maximum value of ε_z^{\max} . The point C , at the same time, should not be above the AB curve, because behind this boundary the technological method does not give a positive result.

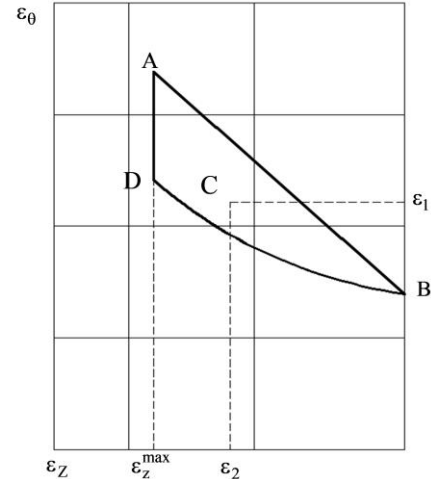


Fig. 11: The curve of the ultimate strains.

The presented theoretical approach allows to describe the forming process of the welded workpiece and to determine the values of the ultimate stresses and deformations in the weld zone.

3.2. The Limiting Degree of Deformation of the Welded Cylindrical Workpieces during the Expansion (Crimping)

Consider, how the weld seam affects to the localization of deformations in the annular layer bordering to the edge of the workpiece. The process of the workpiece with a weld seam expansion is presented in Fig. 12.

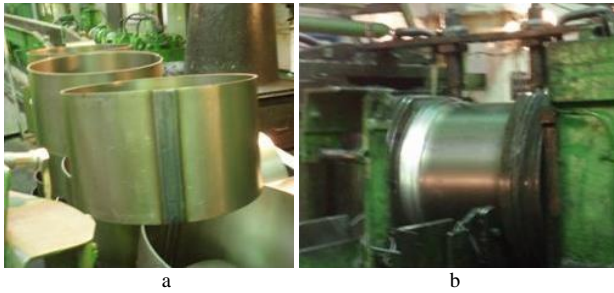


Fig. 12: The expansion process of the welded workpieces: a – view of the workpiece with a weld seam; b – the process of expansion (crimping) of the wheel rim workpiece before the forming

It should be noted that when the annular element is stretched, more pliable elements will begin to deform plastically at the beginning. Usually those elements are located at the weld zone. The deformation will continue until the current yield stress of the weld zone reaches the yield stress of the basic material [9].

The real stresses of the system, workpiece material and the weld seam ratio has the form:

$$\sigma_s = \sigma_B e^{\delta_N} \left(\frac{\delta}{\delta_N} \right)^{\delta_N}, \quad (18)$$

where $\delta_N = \ln \frac{l_N}{l_0}$ is the main logarithmic deformation of elongation before the neck formation beginning in the tensile test;

$\delta = \ln \frac{\rho}{R_0}$ – the main logarithmic deformation of the annular layer

with the ρ coordinate and the workpiece initial radius of R_0 ;

σ_B – tensile strength of the system;

σ_s – yield stress.

The curve of the true stresses of the workpiece material is expressed as:

$$\sigma_s = \sigma_B^M e^{\delta^M}, \quad (19)$$

where σ_B^M is the tensile strength of the workpiece material.

The weld zone hardening law is described as:

$$\sigma_s = \sigma_B^S e^{\delta^S}, \quad (20)$$

where σ_B^S – the tensile strength of the weld zone material;

δ^S – logarithmic deformation of elongation before the neck formation beginning in the tensile test.

The equations (18 – 20) describing the ratios of the tensile or compression strains of the welded workpieces elements.

The system total deformations δ to the weld seam partial deformations δ_s^S ratio:

$$\delta = -\ln \left(\frac{A_{0M}}{e^{\delta^M}} + \frac{A_{0S}}{e^{\delta^S}} \right), \quad (21)$$

where A_{0M} and A_{0S} – the ratio of the initial lengths of the workpiece elements to the initial circumference of the welded workpiece.

The value of δ_K characterizing the ultimate deformation degree during the expansion or crimping is determined by the formula:

$$\delta_K = \left[0,5S_0 - \frac{2}{3}(1 + \delta_s)B \right] / \delta_s B, \quad (22)$$

where $B = R_0 (A_{0M} e^{\delta_{CRIT}} + A_{0S})$;

δ_{CRIT} – the critical degree of deformation, at which less compliant material begins to deform.

The critical degree of deformation is determined as:

$$\delta_{CRIT} = \ln \frac{l_{0S}}{l_{s_{CRIT}}}, \quad (23)$$

where l_{0S} – the initial length of weld seam;

$l_{s_{CRIT}}$ – the weld zone critical length.

The results of calculating of the wheel rims ultimate diameters after expansion and subsequent crimping according to (22) are presented in Table 2.

Table 2: The results of calculating of the wheel rims ultimate diameters after expansion and subsequent crimping

Wheel type	Workpiece diameter D_0 , mm	Ultimate diameter after expansion D_{ULT} , mm
45Ex16	424	456.8
W8-16	424	456.8
DDW18Lx42	982	1103.2
W8-32	816	866
11,75x22,5	539	602.5
DW15Lx38	968	1024
DW15Lx34	867	920

4. Experimental Research Results

The workpieces for all types of experimental work were made from a single sheet, the quality of the material complied with the specifications. After the manufacturing and the heat treatment on the selected regimes, the samples were tested for rupture.

Standard welded samples before and after the failure are shown in Fig. 13.

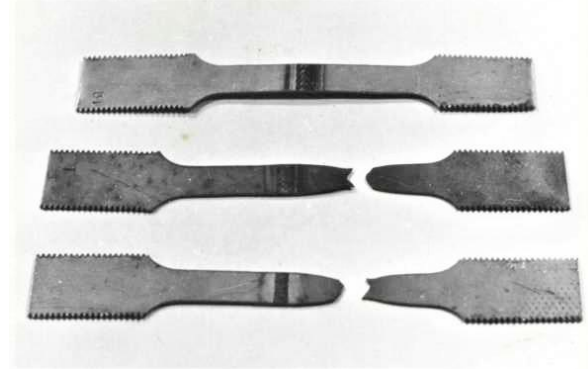


Fig. 13: Welded samples before and after the failure.

During the break tests, standard welded samples were broken not in the weld zone or in the weld seam, but in the basic material. This is due to the coarse grained structure of the weld seam and weld zone, so they have less plasticity than the basic material.

Cylindrical welded workpieces for the experimental works were made from the Steel 08kp and from one sheet in the delivery condition and after its heat treatment. The diameter of the workpieces was 128 mm and the height was 250 mm (Fig. 14).



Fig. 14: Cylindrical sample after stamping.

Changing the height of the samples in the range from 50 to 250 mm and bringing them to the rupture, the results presented in Table 3 were obtained.

Table 3: The results obtained by the samples height varying in the range from 50 to 250 mm, leading to a rupture

Sample No	Sample height		Sample diameter		ϵ_1	$-\epsilon_2$	$-\epsilon_3$
	before the test, H_0 , mm	after the test, H_k , mm	before the test, D_0 , mm	after the test, D_k , mm			
1	250	240.2	128	143	0.112	0.04	0.072
2	200	188.3	128	145	0.126	0.06	0.066
3	170	157.2	128	146.9	0.138	0.078	0.06
4	150	138.3	128	148	0.1455	0.081	0.0645
5	130	119.4	128	148.7	0.1501	0.085	0.651
6	100	91.4	128	149.4	0.155	0.089	0.651
7	70	63.7	128	150	0.159	0.093	0.066
8	50	44.8	128	150.6	0.163	0.108	0.062

Analysis of the experimental data (Table 3) shows that when the cylindrical sample is deformed, the component ϵ_2 has a negative sign. Therefore, at the expansion process of the cylindrical welded workpieces, the material thinness is insignificant and the size along the generatrix decreases while the radial size increases (Fig. 15).



Fig. 15: The samples of wheel rims cylindrical workpieces after test.

The deformations redistribution on both across and along the weld seam was provided by the use of a set of dies with a different sizes of the ellipses semi-axes ratio (Table 4).

Table 4: The results of the deformations ϵ_1 and ϵ_2 redistribution on both across and along the weld seam for different sizes of the semi-axes

No	d_1 , MM	d_2 , MM	d_1 / d_2	ϵ_1	ϵ_2
1	40	40	1	0.148	0.16
2	40	50	1.25	0.144	0.142
3	40	60	1.5	0.127	0.105
4	40	70	1.75	0.119	0.062
5	40	80	2	0.105	0.03
6	40	100	2.5	0.1	0.015

By plotting the test results for the Steel 08kp and the Steel 08ps from Tables 3 and 4, the dependence of $\epsilon_{\theta(1)}$ and $\epsilon_{Z(2)}$ both across and along the weld seam was obtained, at which the welded joint failure occurs (Fig. 16).

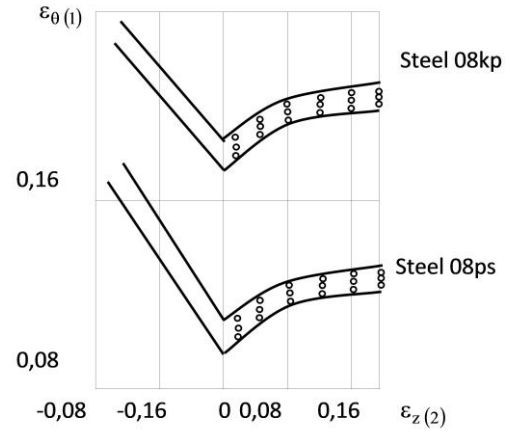


Fig. 16: The curves of the welded joints ultimate deformations for the Steel 08kp and the Steel 08ps.

It can be seen from the graphs in Fig. 16 that the area below the curve is the stamping zone for a material, while the area above the curve is the rupture zone of the welded workpiece. The diagram of the welded joints ultimate deformations consists of two branches: the left one, which corresponds to the cylindrical specimens expansion without flanges clamping, and the right one, which describes the strain change both across and along the weld seam with the clamped flanges.

With a diagram of the welded joint ultimate strains for a specific material, it is possible to predict the possibility of manufacturing a part with a weld seam at the design stage of the process. The experimental data indicate that with the adopted radial-rotational profiling schemes there are practically no reserves for reducing the thickness of the initial workpiece due to significant metal thinning in radius transitions (permissible thinning is 20 – 25 %).

The analysis of the deformations distribution allowed developing, testing and implementing a number of new technological schemes, devices and techniques. Thus, the metal thinning can be significantly reduced, thinner workpiece can be used and thereby a significant reduction in metal consumption can be achieved.

5. Conclusions

1. The most suitable method for calculating the nonstationary stress-strain field for elastoplastic deformation of a cylindrical welded workpieces is the method based on the numerical finite difference modeling of the shaping process.
2. The formalized dependences, which makes it possible to determine the value of the ultimate deformation degree during the welded cylindrical workpieces expansion or crimping is obtained.
3. It is established that with an increase of the workpiece relative thickness and the workpiece and the weld seam materials hardening intensity, the ultimate deformation degree increases.
4. The developed method for calculating a welded cylindrical workpieces made it possible to determine the nonstationary field of stresses and deformations in the deformation region, ultimate deformations and the most rational scheme of the stress-strain state, which excluding the localization of deformations. This ensures the minimum thickness variability of the resulting items and excludes the weld seam and the weld zone destruction.
5. An experimental diagram of the welded workpieces ultimate deformations for the Steel 08kp and the Steel 08ps is obtained, which makes it possible to evaluate the parts with a weld seam manufacture without deformations localization and fracture at the design stage of the technological process.
6. The obtained data allow to predict the plastically deformed materials resistance to fatigue failure and optimize the treatment technology in order to improve the operational properties of metal products.

References

- [1] Pachurin G. V., “Active life of Plastically Processed Steels and Welded Joints”, Forging and stamping production. Material working by pressure, No.12, (2004), pp. 3–8.
- [2] A.A. Shapoval, D.V. Mos’pan, & V.V. Dragobetskii. “Ensuring High Performance Characteristics For Explosion-Welded Bi-metals”, Metallurgist, Vol. 60, Issue 3, (2016), pp. 313–317. doi: 10.1007/S11015-016-0292-9.
- [3] Dragobetskii, V., Shapoval, A., Naumova, E., Shlyk S., Mospan, D., Sikulskiy, V. “The Technology of Production of a Copper – Aluminum – Copper Composite to Produce Current Lead Buses of The High – Voltage Plants”, IEEE International Conference on Modern Electrical and Energy Systems (MEES), (2017), pp. 400–403. doi: 10.1109/MEES.2017.8248944.
- [4] V. Kukhar, V. Artiukh, O. Serdiuk & E. Balalayeva. (2016). Form of gradient curve of temperature distribution of length-wise the billet at differentiated heating before profiling by buckling. *Procedia Engineering*, 165, 1693-1704. doi: 10.1016/j.proeng.2016.11.911.
- [5] Z. Praunseis, T. Sundararajan, M. Toyoda et al. “The influence of soft root on fracture behaviors of high-strength, low-alloyed (hsla) steel weldments”, *Materials and Manufacturing Processes*, Vol. 16, Issue 2, (2001), pp. 229-244 | Published online: 15 Aug 2006. doi: 10.1081/AMP-100104303.
- [6] Z. Praunseis, M. Toyoda, T. Sundararajan. Fracture behaviours of fracture toughness testing specimens with metallurgical heterogeneity along crack front. *Steel res.*, 71, No. 9 (2000).
- [7] V. Sikulskiy, V. Kashcheyeva, Yu. Romanenkov, A. Shapoval. “Study of the process of shape-formation of ribbed double-curvature panels by local deforming”, *Eastern-European Journal of Enterprise Technologies*, Vol. 4, Issue 1 (88) (2017), pp. 43–49. doi: 10.15587/1729-4061.2017.108190.
- [8] Dragobetskii V., Shapoval A., Mos’pan D., Trotsko O., Lotous V. “Excavator bucket teeth strengthening using a plastic explosive deformation”, *Metallurgical and Mining Industry*, No. 4 (2015), pp. 363–368.
- [9] Zagirnyak M., Dragobetskii V., Shapoval O., Mospan D. “The limiting deformation degree of the welded cylindrical blanks during shaping operations of sheet-metal stamping”, *Metallurgical and Mining Industry*, No. 5 (2016), pp. 14 – 21.